Modelling operation parameters of UAV on spray effects at different growth stages of corns

Zheng Yongjun[1], Yang Shenghui[1], Zhao Chunjiang[2], Chen Liping[3], Yubin Lan[4], Tan Yu[1*]

(1. *College of Engineering, China Agricultural University, Beijing 100083, China*;
2. *National Engineering Research Center of Information Technology in Agriculture (NERCITA), Beijing, China*;
3. *National Engineering Research Center of Intelligent Equipment for Agriculture (NERCIEA), Beijing, China*;
4. *College of Engineering, South China Agricultural University, Guangzhou 510642, China*)

Abstract: Currently, unmanned aerial vehicles (UAVs) were widely applied to spray for pest and disease control. However, spray effect can be further improved by setting operation parameters more reasonably and scientifically. Therefore, this study attempts to derive the relationship between operation parameters and spray effect. Different growth stages were distinguished by various corn heights. A six-rotor UAV was operated at different heights and velocities to test pesticides spray effects for corns at different growth stages. Different plant canopy coverage rate and penetrating coefficients were obtained, according to which, the effects on droplet deposition rate caused by different UAVs' operation parameters were analyzed. Droplet penetrating coefficients were applied as indexes to evaluate and select UAVs operation parameters for corns at different growth stages respectively. Mathematical models of droplet penetrating coefficients with UAVs operation parameters were established for corns at all growth stages. The determination coefficients (R^2) of all models were greater than 0.90 and average relative errors were within 20%, which asserted high forecasting accuracy of droplet penetrating rate. With the help of the models, parameters like operating height away from the bottom of corns and UAVs velocities were further analyzed, which guided the optimization of parameter settings and selection of spray methods for corns at different growth stages.

Keywords: multi-rotor unmanned aerial vehicle, spraying, parameter model, growth stage, corn
DOI: 10.3965/j.ijabe.20171003.2578

Citation: Zheng Y J, Yang S H, Zhao C J, Chen L P, Lan Y B, Tan Y. Modelling operation parameters of UAV on spray effects at different growth stages of corns. Int J Agric & Biol Eng, 2017; 10(3): 57–66.

1 Introduction

From huge bell stage to maturity stage, leaf index of corn is between 60 and 100[1]. Every part of corns is easily attacked by diseases like corn curvalaria leaf spot and smut. Moreover, corns are commonly devastated by pests, such as corn aphid, corn borer and armyworm[2,3] in this period. Therefore, the pivotal task of field management is to protect leaves from damage and premature senility to achieve the high yield target. Currently, utilizing terrain machines to spray pesticides is considered as the primary method of chemical pest control. However, in-field operation through applying large machinery can result in leaf damage or even ear drop, which negatively influences the corn growth and production since ridges have been basically sealed.

Research illustrated that droplet penetrating rate and deposition rate are deeply affected by plant shape, volume, leaf area density and physical characteristics[4]. After jointing stage, there is a synchronous extension relationship between stipites elongation and leaf growth

Received date: 2016-01-29 **Accepted date:** 2016-11-22
Biography: Zheng Yongjun, PhD, Associate Professor, research interests: intelligent detection for agriculture machine, Email: zyj@cau.edu.cn; **Yang Shenghui,** Master, research interests: computer measurement and control technology, Email: yang_sheng_h@126.com; **Zhao Chunjiang,** PhD, Research Scholar, research interests: agriculture information technology, Email: zhaocj@nercita.org.cn; **Chen Liping,** PhD, Research Scholar, research interests: intelligent agriculture equipment, Email: chenlp@nercita.org.cn; **Yubin Lan**, PhD, Professor, research interests: agricultural aviation application technique, Email: ylan@scau.edu.cn.

***Corresponding authors: Tan Yu**, PhD, Professor, research interests: intelligent detection and control. College of Engineering, China Agricultural University, Beijing 100083, China. Tel: +86-10-62736385, Email: tanyu@cau.edu.cn.

and unfolding. Moreover, there is a stable and linear relationship between plant height and the number of visible leaves[5,6]. Therefore different growth stages are reflected by different corn heights.

Recently, applying UAVs to achieve low altitude spray is considered as a promising method of disease and pest control. Research mainly focused on the aspects such as working principles of spray components, influences on droplet penetrating rate, coverage rate and recycle rate caused by operation parameters of UAVs as well as appraisal and optimization of spray effect.

Liu et al.[7] reviewed agricultural aviation wind tunnel technology, droplet drift models and measuring methods of droplet distribution range. Ru et al.[8,9] tested droplet deposition and drift by operating an UAV (XY8D) in different operation heights and spray conditions (electrostatic and non-electrostatic). Data were recorded by water sensitive paper and polyester cards, which were analyzed to obtain significance of all the factors to droplet deposition and drift. Similarly, Zhang et al.[10] and other researchers[11-13] operated an UAV (N-3) in different heights, speeds or tree-shapes to analyze different pesticide deposition and drift in non-target areas or fruit trees by verification. Additionally, Guan et al.[14] operated an UAV (CD-10) in a wheat paddock with different operation heights and speeds, and found that spray deposition was negatively related to wind velocity, operation height and speed.

Furthermore, Liao et al.[15] proposed methods for evaluating and optimizing parameters associated in aviation plant protection. Similarly, Sun et al.[16] considered droplet penetration rate, deposition rate and drift rate as independent factors. Optimal outlet air velocities for different plants with different foliage area volume density were derived respectively. The method of estimating UAVs operation speed was proposed and the attenuation model of spray amount within canopies was established. Additionally, regression analyses were performed to study the influences on deposition uniformity caused by operation height, speed and the interaction of height and speed, and fitted models were obtained by Qiu et al.[17,18]

He et al.[19] also researched UAVs application techniques and their impacts on chemical control in Asian rice fields. Droplets depositions were exactly reflected by thermal infrared imager, which helped obtain the optimum operation parameters. Additionally, the effective swath width and uniformity of droplet deposition under headwind flight were tested and coefficients of variation (CVs) of the two airplanes (M-18B and Thrush 510G) were found by Zhang et al.[20], thereby evaluating the performance of spraying systems on the two airplanes.

Regarding researches abroad, UAVs are widely used in different applications. Polo et al.[21] developed an UAV to transport the mobile sensor node to collect data from static sensor nodes in large fields. Moreover, Liénard et al. also applied an UAV to help established 3D models of large objects[22].

More specifically, Endalew et al.[23] established a three-dimension (3D) model for fruit trees and analyzed influences on gas stream of the sprayer caused by wind velocity and direction. Results showed that the maximum jet velocity had a negative relationship with cross wind speed and jet distance but positively related to wind direction. Additionally, Cross et al.[24-26] explored the influence of three factors (air volume of the air blower, atomization quality of sprinkler and sprinkler capacity) on spray effect for apple trees. Moreover, the UAV route was adjusted through evaluating an algorithm, which made the UAV adapt to variations in wind intensity and direction, and the results asserted that the waste of pesticides and fertilizers were significantly reduced[27]. Mesas-Carrascosa et al.[28] programmed various flight missions. Mission planning and image processing were required to be optimized by keeping a balance between spatial resolution and spectral discrimination, thereby achieving agronomic goals.

However, few researchers optimized operation parameters according to real and specific crop conditions (e.g., plant height and density). The aims of this study were to: 1) apply a multi-rotor UAV to spray at different heights and speeds during different corn growth stages; 2) study the relationship between operation parameters (operation height, speed and growth stage) and spray effect; 3) establish models of selecting operation parameters of UAVs for corns at different growth stages, which can improve droplet penetrating and coverage rate

at different plant canopies to achieve the requirement for controlling pests and diseases.

2 Materials and methods

2.1 Experiment materials

2.1.1 UAV and spray system

A remote-control multi-rotor UAV (JF01-10, manufactured by Beijing Weijia Technology Ltd.) was used in the experiments, its main parameters are shown in Table 1.

Table 1 Main parameters of the UAV JF01-10

Parameter	Value	Remark
Flying speed/m·s^{-1}	2, 4, 6	Autonomous set
Flying height/m	1, 1.5, 2	Autonomous set
Main rotor diameter/inch	22	carbon fiber
Size/mm	1780/660/433	Length/width/Height
Mass/kg	15	–
Maximum drug loading/L	10	Maximum capacity
Effective remote control distance/km	1	Effective signal of remote controller

Spray systems consist of pesticide tank, miniature direct current (DC) diaphragm pumps, pipelines and electronic control valves, etc. There are two fan nozzles facing downward and symmetrically deployed on two sides of the UAV. The distance between the two nozzles is 1200 mm. Observed discharge of the entire UAV is 1000 mL/min and droplets' diameters range from 80 μm to 120 μm when nozzle working pressure hits 0.3 MPa.

2.1.2 Droplet collection shelf

As is shown in Figure 1, three horizontal planes were fixed on the top (T), middle (M) and bottom (B) of the vertical stick, on which water sensitive paper was deployed to collect droplets.

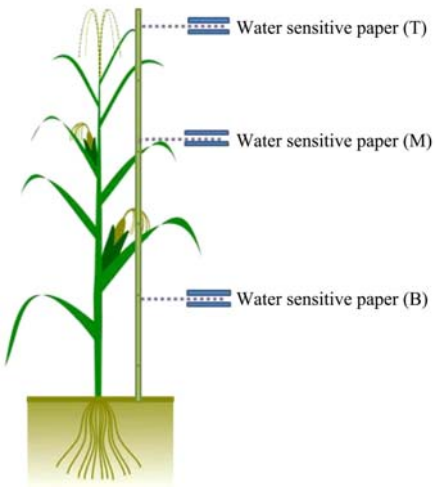

Figure 1 Deployment of water sensitive paper

2.2 Experiment method

In order to study the spray deposition uniformity, test points deployment should be designed. Moreover, methods for monitoring environmental parameters, calculating deposition amount and droplet penetrating coefficient should also be considered.

2.2.1 Site selection and collection shelf deployment

Zhuozhou Experimental Station of China Agricultural University located in Dongchengfang Town in Hebei Province (115.857°E, 39.471°N) was selected as the experimental site. Corns at small bell stage, earing stage and dough stage, with height as 1.20 m, 1.53 m and 2.08 m, respectively, were selected as spray targets.

Experimental site layout is demonstrated in Figure 2. Tests were started from downwind direction and operation area was determined according to parameters of the applied UAV. The flight area was 40 m × 1.5 m. Five droplet collection shelves were deployed at each side of the area with the interval of 5 m and denoted as A_i and B_i (i = 1,2,…,5). The distance between the first and last test points was 20 m, which was half of the entire experimental area length. The start line was set 10 m away from A_1 and B_1, which approximately occupied a quarter of the entire experimental area length, to guarantee enough distance for the UAV to achieve the optimal spray effect. For the same purpose, the distance between every two test points was set as double of field ridge width (0.75 m), which was shorter than the spray span. Relative arms for indicating operation height and flight range were set within the flying zone.

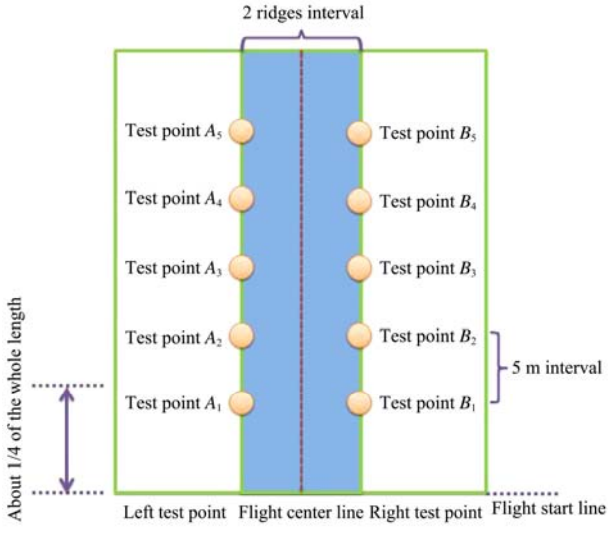

Figure 2 Schematic diagram of the site layout

2.2.2 Monitoring environmental parameters

Average wind speed, temperature and humidity were monitored during the test process; since the duration of a single flight ranged from 7 s to 20 s. The method of monitoring wind speed was based on the method applied by meteorological station. Wind speed in the direction of east, east by north 45° and north were monitored at every test point. Average temperature and humidity were recorded according to the data monitored by meteorological station.

During the tests, the average temperature was 25°C with the highest temperature of 26°C, and relative humidity was 56%. Wind speed in the south was slower than 4 m/s. Wind speed and direction had few influences on every test point since the tests were performed at the downwind area.

2.2.3 Methods of calculating droplet penetration and deposition

The ratio of sprayed area to sampled area of water sensitive paper was defined as the droplet coverage rate, which was selected as the measurement index of droplet deposition. Mean value of droplet coverage rates at all test points was considered as the coverage rate of all canopies (a), which was derived by Equation (1). The number of test points on one side of the test area was denoted as n. Moreover, A_i and B_i were corresponding coverage rates at different test points.

$$a = \frac{1}{n}\sum_{i=1}^{n}(A_i + B_i) \quad (1)$$

The non-uniform coefficient of droplet coverage rate at different canopies was defined as the evaluation index of droplet penetration[29], which was denoted as b and calculated by Equation (2). Strong droplet penetration can be indicated by small b value. The coverage rates at the top, middle and bottom of plants were defined as a_{max}, a_{mid} and a_{min}, respectively, and $\overline{a}$ represents the mean value of these three coverage rates (Equation (3)).

$$b = \frac{a_{max} - a_{min}}{\overline{a}} \quad (2)$$

$$\overline{a} = \frac{1}{3}(a_{max} + a_{min} + a_{mid}) \quad (3)$$

2.2.4 Experiment design

Full factorial design was selected to analyze the influences on droplet penetration caused by operation height and speed. Operation height (h) had three levels: 1.0 m, 1.5 m and 2.0 m. Moreover, the UAV was operated from 2 m/s to 6 m/s with the interval of 2 m/s. Similarly, corn height (H) was also set with three levels: 1.20 m, 1.53 m and 2.08 m. Data from test points (A_1 to A_5) were applied to derive the regression model, which was validated by the data from test points (B_1 to B_5).

The UAV was operated along the central line at a constant speed. Water sensitive paper was collected 30 s after the UAV passing every test point. Furthermore, water sensitive paper was classified according to different plant heights and operation parameters before being scanned by a high resolution scanner.

3 Results and analysis

3.1 Results derived from scanned water sensitive paper

As shown in Figures 3a-3c, water sensitive paper deployed at different heights were scanned in sequence, in which black spots were the areas sprayed by the UAV while yellow areas were non-sprayed areas. The operation parameters were 1.5 m and 2 m/s for Figure 3a, 1.5 m and 4 m/s for Figure 3b, and 2 m with 4 m/s for Figure 3c.

Software developed by Beijing Agricultural Intelligent Equipment Research Centre for analyzing droplet deposition was applied to scan and analyze water sensitive paper to derive coverage rate. The Equation (4) was the mathematical calculation; L was the length of the long edge of the image; W was the length of the short edge of the image; $f(i, j)$ was the pixels with zero grey value.

$$a = \frac{\sum_{i=1}^{L}\sum_{j=1}^{W} f(i,j)}{L \times W} \times 100\% \quad (4)$$

According to Equation (4), the coverage rates of each water sensitive paper were calculated by the software. Data from test points (A_1 to A_5) were recorded and applied to calculate the mean coverage rate at every canopy according to Equation (1). Afterwards, b was derived based on Equation (2) and all results are demonstrated in Table 2.

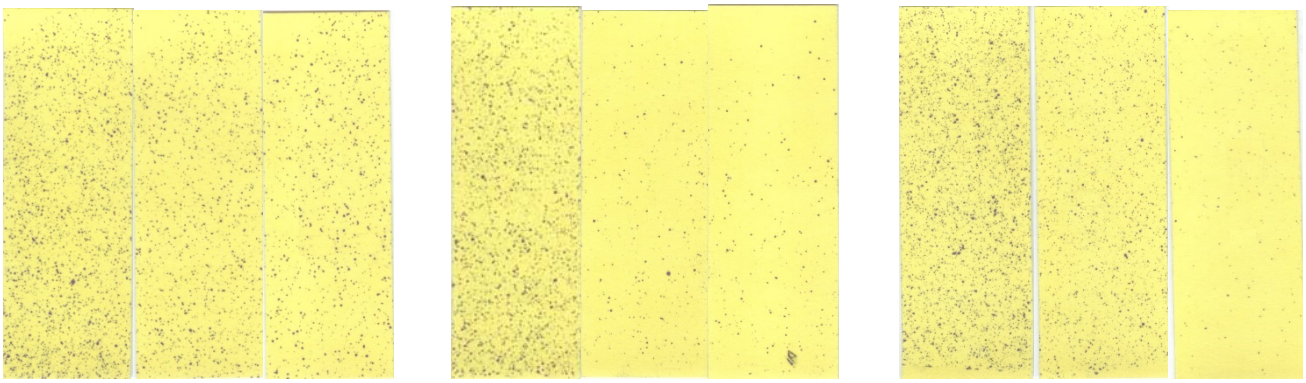

a. One of the results of 1.20 m b. One of the results of 1.53 m c. One of the results of 2.08 m

Figure 3 Scanned water sensitive papers at T, M and B from left to right, respectively

Table 2 Test results of coverage rate

h/m	*H*/m	*V* /m·s^{-1}	Mean coverage rate at top/%	Mean coverage rate at middle/%	Mean coverage rate at bottom/%	*b*
1.2	1	2	5.26	4.38	0.44	1.435948
1.2	1	4	4.85	3.35	2.13	0.792151
1.2	1	6	4.60	1.77	1.57	1.147448
1.2	1.5	2	5.87	2.50	1.72	1.235994
1.2	1.5	4	2.90	2.49	0.74	1.056373
1.2	1.5	6	0.49	0.24	0.08	1.509317
1.2	2	2	4.96	2.36	0.66	1.620452
1.2	2	4	1.29	0.89	0.51	0.869888
1.2	2	6	2.15	1.20	0.58	1.205357
1.53	1	2	2.00	1.29	0.72	0.957606
1.53	1	4	7.46	0.86	0.31	2.485516
1.53	1	6	5.86	4.76	2.03	0.908300
1.53	1.5	2	2.46	2.57	0.30	1.215760
1.53	1.5	4	0.87	0.25	0.23	1.422222
1.53	1.5	6	0.59	0.30	0.17	1.188679
1.53	2	2	1.05	1.08	0.41	0.755906
1.53	2	4	0.98	0.72	0.06	1.568182
1.53	2	6	0.81	0.42	0.09	1.636364
2.08	1	2	8.54	0.08	1.28	2.536364
2.08	1	4	5.21	1.81	1.14	1.496324
2.08	1	6	2.23	0.47	0.49	1.636364
2.08	1.5	2	14.3	5.03	4.60	1.216047
2.08	1.5	4	2.81	1.24	0.90	1.157576
2.08	1.5	6	1.82	1.44	0.07	1.576577
2.08	2	2	9.10	8.13	4.02	0.717176
2.08	2	4	5.49	2.65	0.37	1.804935
2.08	2	6	0.83	0.27	0.09	1.865546

3.2 Data analysis

3.2.1 Effects on droplet coverage rate caused by parameters

Mean coverage rate at different canopies in Table 2 were employed to analyze influences on droplet coverage rate caused by different operation parameters. Relation surfaces of operation speed, height and coverage rate were established by MATLAB, as shown in Figure 4 and 5, which were grouped by plant height. Plant height was 1.20 m, 1.53 m and 2.08 m from top to bottom, respectively. As shown in Figure 4, *X*, *Y* and *Z* axis represented operation speed, canopy height and coverage rate, respectively. Similarly, as demonstrated in Figure 5, relation surfaces of operation height, canopy height and coverage rate were established. *X*, *Y* and *Z* axis represented operation height, canopy height and coverage rate, respectively.

Influences on coverage rate caused by different operation parameters were obtained. As demonstrated in Figure 4, droplet coverage rate reduced when operation speed and canopy height decreased. Besides, droplet coverage rate lowered with the decrease of operation height and canopy height.

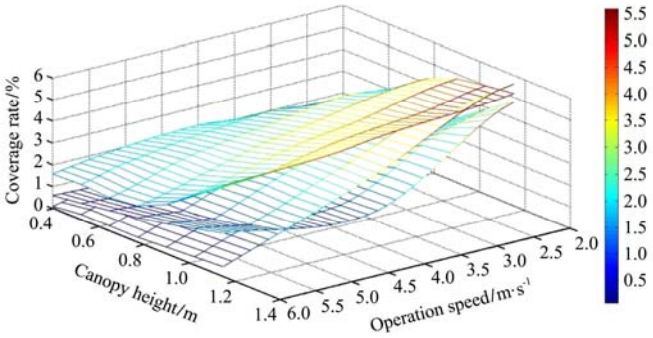

a. Relation surfaces of operation speed, canopy height and coverage rate of plants for small bell stage

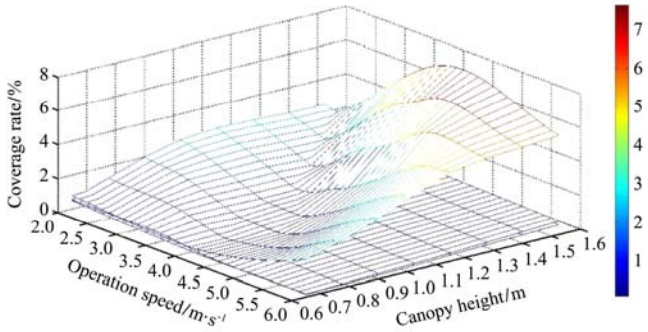

b. Relation surfaces of operation speed, canopy height and coverage rate of plants for earing stage

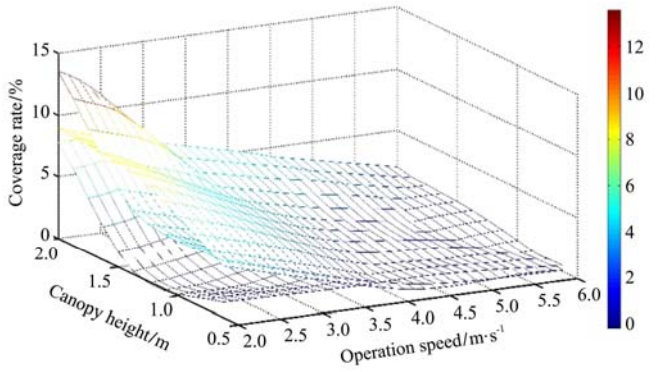

c. Relation surfaces of operation speed, canopy height and coverage rate of plants for dough stage

Figure 4 Relation surfaces of operation speed, canopy height and coverage rate of plants with three heights

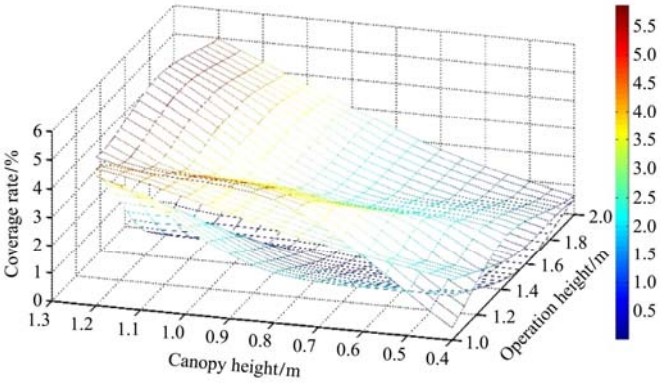

a. Relation surfaces of operation height, canopy height and coverage rate of plants for small bell stage

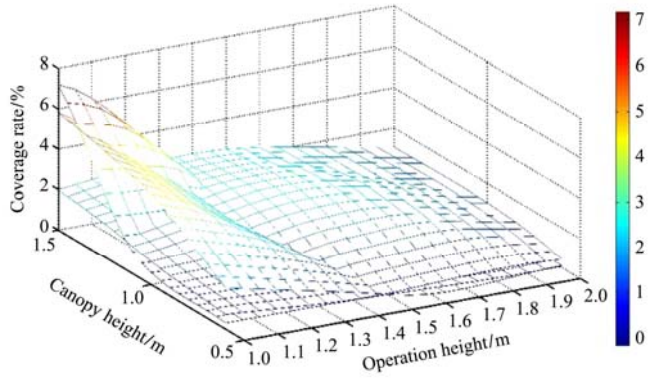

b. Relation surfaces of operation height, canopy height and coverage rate of plants for earing stage

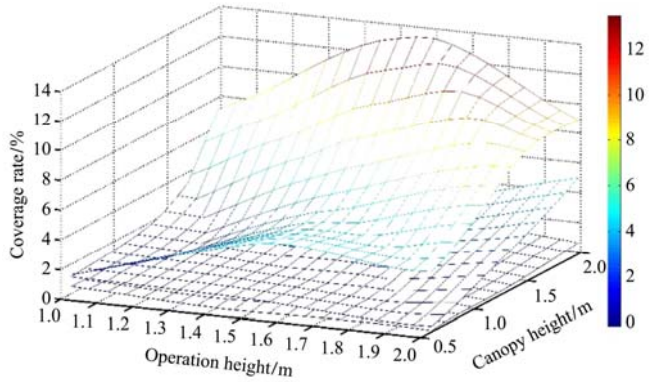

c. Relation surfaces of operation height, canopy height and coverage rate of plants for dough stage

Figure 5 Relation surfaces of operation height, canopy height and coverage rate of plants with three heights

In order to compare effects on coverage rate caused by operation speed and height, coverage rate at the top in Table 2 was subtracted by coverage rate at the bottom. Corresponding difference values are shown in Table 3.

The variation range of difference coverage rate was greater than 3%, which was affected by operation speed since operation height was kept constant. On the contrary, operation height had few effects on coverage rate when operation speed was remained the same. Therefore, operation speed had greater influences on coverage rate for corns with the height of 1.20 m. Operation speed also had greater effects on coverage rate for corns with the height of 1.53 m and 2.08 m.

Table 3 Comparative analysis of operation speed and height

h/m	H/m	v/m·s^{-1}	Difference coverage rate/%
1.20	1	2	4.82
	1	4	2.725
	1	6	3.035
	1.5	2	4.155
	1.5	4	2.155
	1.5	6	0.405
	2	2	4.305
	2	4	0.78
	2	6	1.575

3.2.2 Effects on droplet penetration caused by parameters

Three-dimension surfaces of b, v and h were drawn by MATLAB as shown in Figure 6, in which, X,Y and Z represented operation height, speed and droplet penetration coefficient, respectively.

As demonstrated in Figure 6, droplet had great penetration coefficient when the UAV was operated in the speed and height of 3.5-4.5 m/s and 1.0-1.2 m to spray corns with the height of 1.20 m. Specifically, b achieved the minimum value of 0.792 with the operation speed and height of 4 m/s and 1.0 m, which meant that droplets had the greatest penetration. For plants with the height of 1.53 m, droplet had well penetration with the operation speed and height of 2-3 m/s and 1.8-2.0 m. More specifically, the strongest droplet penetration was reflected by the minimum b (0.755906) with the operation height and speed of 2.0 m and 2 m/s, respectively. Furthermore, for plants with the height of 2.08 m, UAV should be operated with the operation speed and height of 2-3 m/s and 1.8-2.0 m, respectively. Similarly, the optimal operation height and speed was

also 2.0 m and 2 m/s, respectively, to achieve the best droplet penetration, which was reflected by the minimum *b* (0.717176).

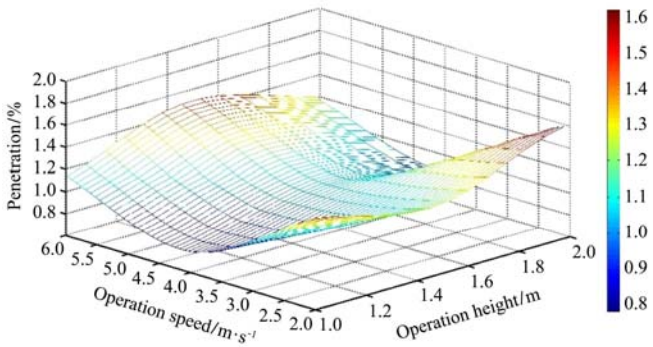

a. Relation surfaces of operation height, operation speed and penetration for small bell stage

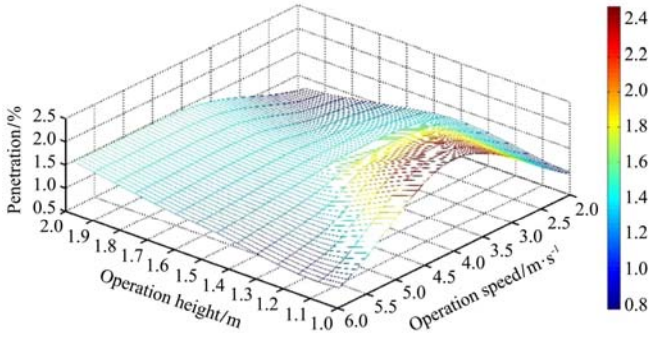

b. Relation surfaces of operation height, operation speed and penetration for earing stage

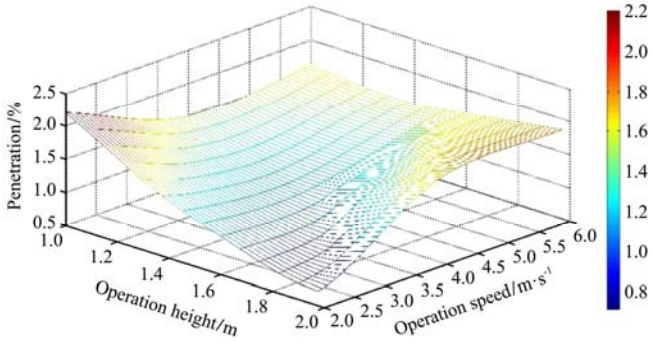

c. Relation surfaces of operation height, operation speed and penetration for dough stage

Figure 6 3-D surfaces of experimental data

Therefore, the optimal operation parameters varied with different plant heights. Corns with the height of 1.20 m mainly at the little bell stage, have the smallest leaf density. However, leaves grow fast and leaf density changes greatly every day at this stage. In addition, corns with the height of 1.53 and 2.08 m mainly at heading and ripening stages, which have high leaf density but leaves grow slowly and leaf density variance is small. Moreover, droplet penetration is related to plant growth stage as mentioned before, which may affect the selection of operation parameters.

4 Models of droplet penetration and operation parameters

Models were established according to the data in Table 2 to quantitatively analyze the effects on droplet penetration caused by different operation heights and speeds.

4.1 Common multiple non-linear regression models

Different types of multiple non-linear regression models are demonstrated in Table 4[30], according to which, the most suitable model was selected.

4.2 Model selection and optimization

Models in Table 4 should be fitted as shown in Figure 7 to derive the most suitable model for this project. Firstly, residual distribution chart should be analyzed. If there were no outliers and the fitted model met the statistical requirements, the selected model suited the project. Otherwise, outliers should be removed and then the model should be fitted again. The model suited the project if statistic requirements were satisfied. However, if the model only met statistical requirements after removing more than two outliers, the model was still considered to be unsuitable[28].

According to the flow chart shown in Figure 7, for corns with the height of 1.20 m, models in Table 4 were fitted in sequence. Significant level (α) was set at 0.05 and the derived test statistics of fitted models are demonstrated in Table 5.

Table 4 Common models of multiple nonlinear regression

Model ID	Model name	Function expression	Transformed linear model
Model 1	Power model	$y = b_1 x_1^{b_2} x_2^{b_3} x_3^{b_4}$	$\ln y = \ln b_1 + b_2 \ln x_1 + b_3 \ln x_2 + b_4 \ln x_3$
Model 2	Growth model	$y = e^{b_1 + b_2 x_1 + b_3 x_2 + b_4 x_3}$	$\ln y = b_1 + b_2 x_1 + b_3 x_2 + b_4 x_3$
Model 3	Logarithmic model	$\ln y = b_1 + b_2 \ln x_1 + b_3 \ln x_2 + b_4 \ln x_3$	—
Model 4	Compound model	$y = b_0 b_1^{x_1} b_2^{x_2} b_3^{x_3}$	$\ln y = \ln b_0 + x_1 \ln b_1 + x_2 \ln b_2 + x_3 \ln b_3$
Model 5	Multiple quadratic model	$y = b_0 + b_1 x_1 + b_2 x_2 + b_3 (x_1 + x_2)^2$	—

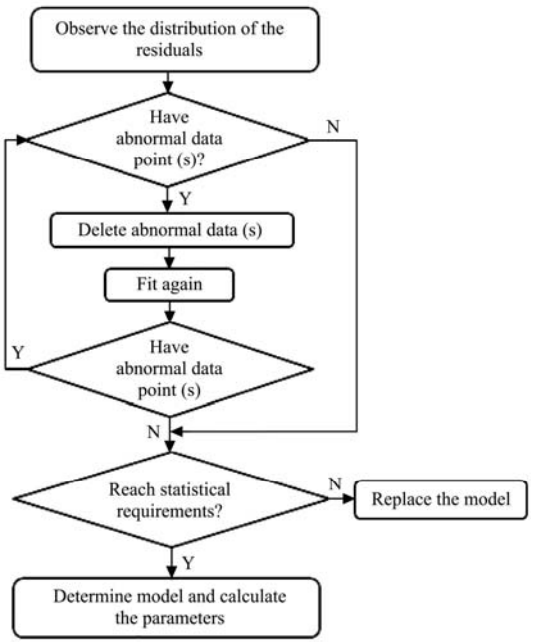

Figure 7 Flow chart of fitting model

Table 5 Parameter comparison of fitted models

Model ID	R^2	F-value	p-value	Relative estimation error variance (S)
Model 1	0.1297	0.4471	0.6592	0.0678
Model 2	0.0615	0.1964	0.8267	0.0731
Model 3	0.1480	0.5210	0.6186	0.0891
Model 4	0.0615	0.1924	0.8267	0.0731
Model 5	0.4427	1.3239	0.3648	0.0699

As shown in Table 5, model 5 had the greatest R^2 (0.4427), which was selected for this project. However, the R^2 of the original model was far to one, which was required to be optimized. The influence of the cross term on the penetration should be considered. Therefore, model 5 was improved as following:

$$y = b_0 + b_1x_1 + b_2x_2 + b_3(x_1 + x_2)^2 \quad (5)$$

The coefficients of each term were staged different with each other in Equation (5) and replaced by specific variables as following:

$$b = b_0 + b_1h + b_2v + b_3vh + b_4h^2 + b_4v^2 \quad (6)$$

The optimized model of Equation (6) was fitted and the residual distribution chart was demonstrated in Figure 8. There was an outlier, which was required to be removed to derive the residual distribution chart without outliers. As shown in Figure 9, residuals were near to the central line and symmetrically distributed around the central line, which asserted that the original data can be represented by the fitted model.

Coefficients in Equation (6) were calculated by MATLAB and results are shown as follows:

$[b_0, b_1, b_2, b_3, b_4, b_5]$ = [0.7566, 3.5829, –1.1323, –0.0316, –1.1165, 0.1370]

Bint = [–0.8042, 2.3175, 1.4198, 5.7459, –1.4850, –0.7797, –0.1335, 0.0702, –1.8224, –0.4106, 0.0988, 0.1753]

stats = 0.9928, 55.4739, 0.0178, 0.0022

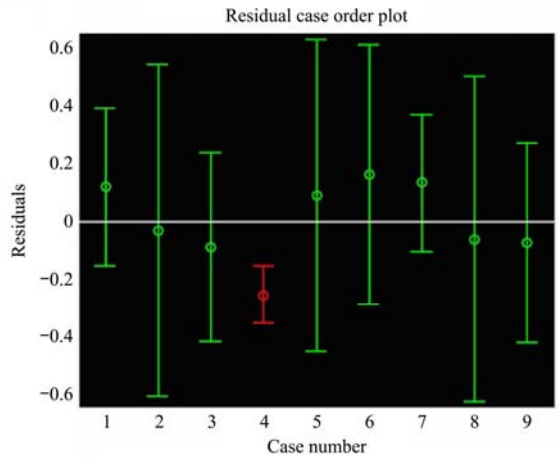

Figure 8 Residual distribution with outliers

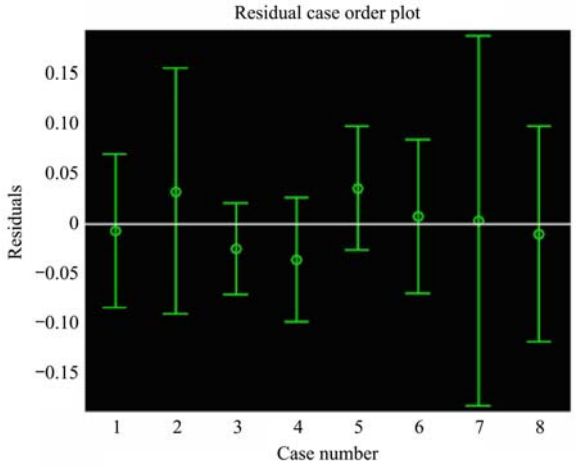

Figure 9 Residual distribution without outliers

The original data could be represented by the fitted model since R^2 was close to one (0.9928). Moreover, the fitted model had great significance (p=0.0178<0.05). Therefore, values of h and v were substituted into the fitted model to derive theoretical values demonstrated in Table 6.

According to Table 6, relative errors were small after removing the outlier, which guaranteed high reliability and feasibility of the fitted model. Therefore, coefficients can be substituted into the model to derive Equation (7), which was suitable for corns with the height of about 1.20 m.

$$b = 0.7566 + 3.5829h - 1.1324v - 0.0316vh - 1.1165h^2 + 0.137v^2 \quad (7)$$

Similarly, models for corns with the height of about 1.53 m and 2.08 m were also derived as shown in Equations (8) and (9), respectively.

$$b = 0.9155 - 1.3471h + 0.5524v + 0.2324vh + 0.2238h^2 - 0.0999v^2 \quad (8)$$

$$b = 5.9194 - 3.5275h - 0.983v + 0.3652vh + 0.5251h^2 + 0.0669v^2 \quad (9)$$

Table 6 Comparison of theoretical and measured values for corns with the height of 1.20 m

Theoretical values	Measured values	Relative errors/%
1.443	1.435948	0.4911
0.759	0.792151	–4.1850
1.171	1.147448	2.0526
1.0916	1.056373	3.3348
1.472	1.509317	–2.4724
1.6132	1.620452	–0.4475
0.866	0.869888	–0.4470
1.2148	1.205357	0.7834

4.3 Model verification

The established model was verified by comparison of the measured value and the theoretical value of *b*, which was represented by relative errors. Experimental results of corns with the height of 1.20 m at B_1-B_5 were demonstrated in Table 7, in which all relative errors were smaller than 20%.

Table 7 Experimental results of corns with the height of 1.20 m at B_1-B_5

Theoretical values	Measured values	Relative errors/%
1.443	1.411295	2.25
0.759	0.806673	–5.91
1.171	1.258514	–6.95
1.8072	1.563003	15.62
1.0916	1.116012	–2.19
1.6132	1.730938	–6.80

Table 8 Experimental results of corns with the height of 1.53 m at B_1-B_5

Theoretical values	Measured values	Relative errors/%
0.534435	0.49153	8.73
2.013369	2.143556	–6.07
1.612266	1.66472	–3.15
1.703093	1.903414	–10.52
1.32874	1.278571	3.92
1.900621	2.0	–4.97

The experimental results of corns with the height of 1.53 m and 2.08 m at B_1-B_5 are shown in Table 8 and Table 9, respectively.

Relative errors may be caused by assumptions (e.g., fluctuation of wind speed and different operation habits, etc.) while establishing models. All relative errors were within the allowable range (20%), which guaranteed predictive ability of the model.

Table 9 Experimental results of corns with the height of 2.08 m at B_1-B_5

Theoretical values	Measured values	Relative errors/%
1.949	2.389108	–18.42
1.5162	1.751748	–13.45
1.6186	1.84193	–12.12
1.6068	1.564885	2.68
1.0248	1.045455	–1.98
1.8576	1.785047	4.06

5 Conclusions

The multi-rotor UAV was operated at different heights and speeds to spray corns at different growth stages respectively for investigating the effects of operation parameters on droplet penetrability and coverage rate. The models of surfaces and calculating droplet penetrability coefficients were established with operation height and flying speed as independent variables. According to the models, the optimal operation parameters were 1 m and 4 m/s for small bell stage corn, 2 m and 2 m/s for both earing stage and dough stage corns. Moreover, it could be known that the flying speed had greater influence on droplet coverage rate than operation height. The R^2 of the mathematical models was greater than 0.9, which asserted high reliability and predictive ability of the models.

Acknowledgements

This research was supported and funded by The National Key Research and Development Program of China (No. 2016YFD0200700) from Ministry of Science and Technology, and the Chinese Universities Scientific Fund under Grand No. 2017QC139 & No. 2017GX001, and helped by VIGA UAV Company (Beijing).

[References]

[1] An W, Fan Z X, Yang S C, Mi X H, Ma H L, Wang J H, et al. Corresponding relationship of maize leaf age index, ear differentiation and shape. Journal of Shanxi Agricultural Sciences, 2005; 33(4): 41-43. (in Chinese)

[2] Chen X H. Occurrence and prevention of common diseases in maize growth. Agriculture and Technology, 2015; 35(12): 20. (in Chinese)

[3] Liu T J. Comprehensive prevention and control measures of three common diseases of corn. Jilin Agriculture, 2012; 6:

71. (in Chinese)

[4] Song S R, Hong T S, Wang W X, Zhang H X, Luo X W, Sévila F. Testing analysis on deposit and distribution of pesticide spraying in rice fields. Transactions of the CSAM, 2004; 35(6): 90–93. (in Chinese)

[5] Robertson M J. Relationships between internode elongation, plant height and leaf appearance in maize. Field Crops Research, 1994; 38: 135–145.

[6] Yao Y S, Luo X L, Wang B K, Dai J Y. Studies on simulation of corn morphology growth. Journal of Maize Sciences, 2000; 8: 30–32. (in Chinese)

[7] Liu H S, Lan Y B, Xue X Y, Zhou Z Y, Luo X W. Development of wind tunnel test technologies in agricultural aviation spraying. Transactions of the CSAE, 2015; 31(Z2): 1–10. (in Chinese)

[8] Ru Y, Jin L, Jia Z C, Bao R, Qian X D. Design and experiment on electrostatic spraying system for unmanned aerial vehicle. Transactions of the CSAE, 2015; 31(8): 42–47. (in Chinese)

[9] Ru Y, Jin L, Zhou H P, Jia Z C. Performance experiment of rotary hydraulic atomizing nozzle for aerial spraying application. Transactions of the CSAE, 2014; 30(3): 50–55. (in Chinese)

[10] Zhang S C, Xue X Y, Qin W C, Sun Z, Ding S M, Zhou L X. Simulation and experimental verification of aerial spraying drift on N-3 unmanned spraying helicopter. Transactions of the CSAE, 2015; 31(3): 87–93. (in Chinese)

[11] Xue X Y, Tu K, Qin W C, Lan Y B, Zhang H H. Drift and deposition of ultra-low altitude and low volume application in paddy field. Int J Agric & Biol Eng, 2014; 7(4): 23–28.

[12] Xue X Y, Qin W C, Sun Z, Zhang S C, Zhou L X, Wu P. Effects of N-3 UAV spraying methods on the efficiency of insecticides against planthoppers and Cnaphalocrocis medinalis. Acta Phytophylacica Sinica, 2014; 30(3): 273–278.

[13] Zhang P, Deng L, Lyu Q , He S L, Yi S L, Liu Y D, et al. Effects of citrus tree-shape and spraying height of small unmanned aerial vehicle on droplet distribution. Int J Agric & Biol Eng, 2016; 9(4): 45–52.

[14] Guan X P. Effects of operating parameters for unmanned aerial vehicles on spraying deposition. Hubei Agricultural Sciences, 2014; 53(3): 678–680. (in Chinese)

[15] Liao J, Zang Y, Zhou Z Y, Luo X W. Quality evaluation method and optimization of operating parameters in crop aerial spraying technology. Transactions of the CSAE, 2015; 31(Z2): 38–46. (in Chinese)

[16] Sun C D, Qiu W, Ding W M, Gu J B. Parameter optimization and experiment of air-assisted spraying on pear trees. Transactions of the CSAE, 2015; 24(31): 30–38. (in Chinese)

[17] Qiu B J, Wang L W, Cai D L, Wu J H, Ding G R, Guan X P. Effects of flight altitude and speed of unmanned helicopter on spray deposition uniform. Transactions of the CSAE, 2013; 29(24): 25–32. (in Chinese)

[18] He X K, Liu Y J, Song J L, Zeng A J, Zhang J. Small unmanned aircraft application techniques and their impacts for chemical control in Asian rice fields. Aspects of Applied Biology, 2014; 122: 33–45.

[19] Qin W C, Qiu B J, Xue X Y, Chen C, Xu Z F, Zhou Q Q. Droplet deposition and control effect of insecticides sprayed with an unmanned aerial vehicle against plant hoppers. Crop Protection, 2016; 85: 79–88

[20] Zhang D Y, Chen L P, Zhang R R, Wesley C H, Xu G, Lan Y B. Evaluating effective swath width and droplet distribution of aerial spraying systems on M-18B and Thrush 510G airplanes. Int J Agric & Biol Eng, 2015; 2(8): 21–30.

[21] Polo J, Hornero G, Duijneveld C, García A, Casas O. Design of a low-cost wireless sensor network with UAV mobile node for agricultural applications. Computers and Electronics in Agriculture, 2015; 119: 19–32.

[22] Liénard J, Vogs A, Gatziolis D, Strigul N. Embedded, real-time UAV control for improved, image-based 3D scene reconstruction. Measurement, 2016; 81: 264–269.

[23] Endalew A M, Debaer C, Rutten N, Vercammenb J, Delelea M A, Ramona H, et al. A new integrated CFD modelling approach towards air-assisted orchard spraying. Part I. Model development and effect of wind speed and direction on sprayer airflow. Computers and Electronics in Agriculture, 2010; 71(2): 128–136.

[24] Cross J V, Walklate P J, Murray R A, Richardson G M. Spray deposits and losses in different sized apple trees from an axial fan orchard sprayer: 1. Effects of spray liquid flow rate. Crop Protection, 2001; 20(1): 13–30.

[25] Cross J V, Walklate P J, Murray R A, Richardson G M. Spray deposits and losses in different sized apple trees from an axial fan orchard sprayer: 2. Effects of spray quality. Crop Protection, 2001; 20(4): 333–343.

[26] Cross J V, Walklate P J, Murray R A, Richardson G.M. Spray deposits and losses in different sized apple trees from an axial fan orchard sprayer: 3. Effects of air volumetric flow rate. Crop Protection, 2003; 22(2): 381–394.

[27] Faical B S , Costa F G, Pessin G, Jo U, Heitor F, Alexandre C, et al. The use of unmanned aerial vehicles and wireless sensor networks for spraying pesticides. Journal of Systems Architecture, 2014; 60(4): 393–404.

[28] Mesas-Carrascosa F J, Torres-Sanchez J, Clavero-Rumbao I, García-Ferrer A, Peña-Barragán J M, Irene B S, et al. Assessing optimal flight parameters for generating accurate multispectral orthomosaicks by UAV to support site-specific crop management. Remote Sensing, 2015; 7(10): 12793–12814.

[29] Zhang T. Experimental study and CFD simulation of air-assisted system on super-high clearance boom sprayer. Beijing: Chinese Academy of Agricultural Mechanization Sciences, 2012; pp.1–132. (in Chinese)

[30] Deng Y P, Zhou B, Liu Y J, Wang J, Guo P J. Research on mathematical modeling of experimental data. Marine Technology, 2006; 3(3): 19–22.